energies

MDPI

Article

Experimental Investigation of Graphene Nanoplatelets Enhanced Low Temperature Ternary Eutectic Salt Hydrate Phase Change Material

B. Kalidasan [1], A. K. Pandey [1,2,*], Saidur Rahman [1], Kamal Sharma [3] and V. V. Tyagi [4]

[1] Research Centre for Nano-Materials and Energy Technology (RCNMET), School of Engineering and Technology, Sunway University, Petaling Jaya 47500, Malaysia
[2] Center for Transdisciplinary Research (CFTR), Saveetha Institute of Medical and Technical Services, Saveetha University, Chennai 602105, India
[3] Department of Mechanical Engineering, Institute of Engineering and Technology, GLA University, Mathura 281406, India
[4] School of Energy Management, Shri Mata Vaishno Devi University, Katra 182320, India
* Correspondence: adarshp@sunway.edu.my

Abstract: A sustainable approach to ensuring the thermal regulation of space is reliable with phase change materials (PCMs) operating at 15–25 °C. Henceforth, there is a need of a search of binary and ternary eutectic PCMs operating at desirable phase transition temperatures of 15–25 °C, high energy storage enthalpy (180–220 J/g), improved thermal conductivity and better absorptivity of solar energy. In this current research, we developed a ternary eutectic inorganic salt hydrate PCM intended for a low-temperature thermal regulation system. Based on the eutectic melting point theory, the phase transition temperature and proportion of sodium carbonate decahydrate (SCD), sodium phosphate dibasic dodecahydrate (SPDD) and sodium sulphate decahydrate (SSD) were determined. As per the calculated proportion, ternary eutectic PCM was experimentally prepared. Furthermore, to enhance the thermal property, graphene nanoplatelets (GNP) were dispersed at weight concentrations of 0.4%, 0.7% and 1.0%. The prepared nanoparticle-dispersed PCMs were characterized using an optical microscope, Fourier transform infrared (FT-IR) spectroscopy and a thermal conductivity meter, and a differential scanning calorimeter (DSC) was used to evaluate the morphology, chemical stability and thermal properties. The results showed increases in thermal conductivity and optical absorbance by 71.5% and 106.5%, respectively, with GNP at 1.0% weight concentration. Similarly, the degree of supercooling and transmissibility was reduced by 43.5% and 76.2% correspondingly. The prepared composite PCM is expected to contribute towards cooling, with an intention to contribute towards sustainable development.

Keywords: salt hydrate; phase change materials; graphene nanoplatelets; thermal energy storage

check for updates

Citation: Kalidasan, B.; Pandey, A.K.; Rahman, S.; Sharma, K.; Tyagi, V.V. Experimental Investigation of Graphene Nanoplatelets Enhanced Low Temperature Ternary Eutectic Salt Hydrate Phase Change Material. *Energies* **2023**, *16*, 1574. https://doi.org/10.3390/en16041574

Academic Editor: Ann Lee

Received: 4 January 2023
Revised: 30 January 2023
Accepted: 31 January 2023
Published: 4 February 2023

Copyright: © 2023 by the authors. Licensee MDPI, Basel, Switzerland. This article is an open access article distributed under the terms and conditions of the Creative Commons Attribution (CC BY) license (https://creativecommons.org/licenses/by/4.0/).

1. Introduction

The desire to resolve the problem of excess carbon emissions that cause global warming and serious environmental threats has led to developing and utilizing clean and renewable energy sources. Due to the intermittent nature of renewable energy sources like solar, wind and hydropower, there exists an imbalance between the energy demand and supply. Based on the active research over the past decade, it is observed that thermal energy storage (TES) systems are more likely to resolve the mismatch of energy supply and demand by effectively utilizing solar energy. Among the three (latent heat storage, sensible heat storage and chemical heat storage) [1] general categories of TES techniques we would focus more on latent heat storage. The benefits of latent heat storage using phase change materials (PCMs) are more reliable as they need neither to be controlled as in the case of chemical heat storage nor undergo the hindrance of less energy density as in sensible

heat storage. Based on the composition, PCMs are mainly categorized as organic (paraffin, fatty acids and sugar alcohols), inorganic (salt hydrates) and eutectic (mixture of organic–organic, organic–inorganic or inorganic–inorganic) [2]. A few notable hindrances with organic PCMs are low thermal conductivity, flammable nature and high cost. In the case of inorganic PCMs, their thermal conductivity is high compared to that of organic PCMs, they are non-flammable, have larger energy storage density and are cheaper [3]. Eutectic PCMs are a tailored material, where the melting point and the thermal property of the PCM are designed as per the designated application. Due to the non-flammable and economic benefit of inorganic PCMs, they are more preferred for space (building) heating and cooling, solar water heating systems, waste heat recovery units and in energy regulation units.

Considering the advantage of eutectic PCMs in formulating the eutectic composition as per the requirement of energy storage application, numerous research works have been carried out. A few outstanding contributions are discussed briefly to identify and elaborate the uniqueness of the current research work. Cheng et al. [4] conducted an experimental investigation with a ternary eutectic nitrate composite PCM $LiNO_3.3H_2O - KNO_3 - NaNO_3$ by dispersing expanded graphite nanoparticles. The results showed a maximal melting enthalpy of 159 J/g with thermal conductivity of 4.565 W/m·K with 20% of modified expanded graphite nanoparticles. Although the phase transition temperature of the developed ternary composite PCM was 21.66 °C, the heat storage enthalpy was much lower. Like in the previous work, Tian et al. [5] developed a ternary eutectic carbonate salt operating at a very high temperature of 725 °C. The composite mixture of the ternary salt was $(Li_2CO_3 - Na_2CO_3 - K_2CO_3)$ with heat of fusion equal to 160 J/g. Based on Gibbs energy of fusion, Wang et al. [6] developed a high-temperature (420 °C) ternary eutectic PCM with salts of $LiF - Na_2CO_3 - K_2CO_3$. The designed high-temperature ternary PCM was applied for heat transfer fluid for effective TES. Liang and Chen et al. [7] developed a ternary eutectic PCM $(K_2HPO_4.3H_2O - NaH_2PO_4.2H_2O - Na_2S_2O_3.5H_2O)$ for cold storage application operating at a temperature of −14 °C, with latent heat capacity of 127 J/g. The research investigation was focused on the role of thickening and nucleating agents in resolving the phase instability and the supercooling issue. Sun et al. [8] conducted a TES experiment for buildings by developing a ternary eutectic salt hydrate mixture using 95% of $CaCl_2.6H_2O$, 4% of NH_4Cl and 1% of $SrCl_2.6H_2O$ with a phase transition temperature of 23.5 °C. In another research work, a ternary eutectic PCM was developed for air conditioning and building cooling [9]. The ternary eutectic PCM $(Zn(NO_3)_2.6H_2O - Mn(NO_3)_2.4H_2O - KNO_3)$ was designed to operate at 20 °C with a melting enthalpy of 110 J/g. This investigation also focused on determining the right nucleating agent for the developed PCM.

In other work, Zhang et al. [10] developed a lauric–myristic–palmitic acid ternary eutectic PCM at a eutectic mixture proportion of 55.24/29.74/15.02 operating at a temperature of 31.5 °C. To further enhance the thermophysical property, they expanded the graphite nanoparticles' weight concentration to 5.5% and achieved thermal conductivity of 1.67 W/m·K with compensation in latent heat. An organic-PCM-based ternary eutectic composite operating at a phase transition temperature of 17 °C was developed with 64.8% capric acid, 22.6% myristic acid and 12.6% palmitic acid [11]. Melting latent heat and thermal conductivity of the developed CA–MA–PA ternary eutectic PCM were 131.7 J/g and 0.149 W/m·K, respectively. To further enhance the thermal performance, 10% exfoliated graphite was dispersed and resulted in an increase of thermal conductivity to 20% with compensating the heat storage ability. Similarly, in another research work [12], a ternary eutectic composite of capric acid, palmitic acid and stearic acid was investigated by dispersing expanded vermiculite at a 30% weight concentration. The developed ternary eutectic PCM CA–PA–SA was designed to operate at a temperature of 19.3 °C with melting enthalpy of 117 J/g. For its thermal stability and noncorrosive properties, Ke et al. [13] developed a fatty-acids-based ternary eutectic PCM. Ternary eutectic PCMs were opted based on his earlier research work and were (a) CA–LA–PA (63.37/31.56/5.07), (b) CA–LA–SA (65.32/32.54/2.14), (c) CA–MA–PA (71.82/18.86/9.32), (d) CA–MA–SA (72.65/21.17/6.18) and (e) CA–PA–SA (83.82/10.19/5.99). The melting point and latent heat values of all

the prepared form-stable PCMs were determined to be 15–35 °C and 120–139 J/g correspondingly. Luo et al. [14] developed a form-stable ternary eutectic PCM by impregnation (CA–PA–SA) into nano SiO_2. The developed form-stable ternary PCM was designed to operate at the temperature range of 17–26 °C with latent heat of 100 J/g. The intended application of the PCM was to store solar radiation and provide better thermal regulation of a building during the winter season. He et al. [15] developed two ternary eutectic PCMs with (a) lauric–myristic–palmitic acid (59/26/15) and (b) lauric–myristic–paraffin (51/28/21) operating at melting points of 32.3 °C and 31.5 °C. The enthalpies of the developed ternary PCMs were 160 J/g and 172 J/g, respectively. Based on the current literature analysis, it can be inferred that most of the developed low eutectic PCMs are used directly in various TES applications without inclusion of any further additives or nanomaterials. Likewise, a recent advancement in material science has led to the usage of carbon-based nanomaterials with higher thermal conductivity to be dispersed with the base PCM for enhancing the thermal property. Depending on the unique shape and structure, carbon nanomaterials are of 1D, 2D and 3D. Among them, 2D graphene nanoplatelets and nanomaterials offer better thermal enhancement due to higher specific surface area, ability to better accommodate foreign materials at the gaps of layers, and higher thermal conductivity. The major focus of the research work was to experimentally compare their performance with respect to the number of thermal cycling over a longer duration of operation. In the literature it can be found that the predominantly used PCM for developing a new ternary eutectic PCM was organic fatty acids, and there is a void of research works performed with inorganic PCMs, especially with low-temperature salt hydrates.

The current research investigation focuses on the design and development of a low-temperature ternary eutectic PCM with a mixture of inorganic salt hydrate sodium carbonate decahydrate (SCD), sodium phosphate dibasic dodecahydrate (SPDD) and sodium sulphate decahydrate (SSD). The ternary eutectic mixture proportion and melting point of SCD/SPDD/SSD PCM was designed using Schrader's equation, followed by experimental synthesis and analysis of their thermal properties. Melting (21.3 °C) and latent heat values (202.2 J/g) of the ternary eutectic PCM determined using differential scanning calorimetry (DSC) were in accordance with the numerically calculated values (T_m = 21.5 °C and ΔH_m = 207 J/g) at the eutectic mixture. It was detected that graphene nanoplatelets (GNPs) exhibited a two-dimensional flat and thin plate-like structure with high surface area. GNP nanomaterials are unsystematically organized with spacing between alternate layers that enhance the intermolecular force of attraction when dispersed with a eutectic composite. GNPs are more likely to contribute to the base ternary eutectic salt hydrate PCM by improving the thermophysical characteristics, particularly (a) melting enthalpy, (b) conductive nature by developing thermal networks and (c) enhanced optical absorptivity of solar radiation owing to the dark appearance. For further enhancement of thermal properties, the developed ternary eutectic PCM SCD/SPDD/SSD were dispersed with GNP to prepare three composite mixtures at weight concentrations of 0.4%, 0.7% and 1.0%. Chemical stability using Fourier transform infrared spectroscopy (FT-IR), optical absorptivity using ultraviolet visible spectroscopy (UV–vis), thermal conductivity using thermal hot bridge instrument and thermophysical properties like melting point, latent heat storage and degree of supercooling using a DSC instrument were characterized. Finally, to analyze the heat transfer rate between the developed ternary eutectic PCM and the GNP-dispersed ternary eutectic PCM, a numerical simulation using ANSYS software was conducted based on their thermal conductivity with variation in heat input. The developed ternary eutectic PCM was expected to improve the application of the inorganic salt hydrate PCM for thermal regulation of buildings and is more likely to contribute to the Sustainable Development Goals (SDGs)

2. Materials and Methods

2.1. Materials

The salt hydrates PCMs used in the current research investigations were sodium carbonate decahydrate (SCD), sodium sulphate decahydrate (SSD) and sodium phosphate dibasic dodecahydrate (SPDD). All the three inorganic salt hydrate PCMs, SCD with T_m 31 °C, SSD with T_m 33 °C and SPDD with T_m 37 °C were procured from Sigma Aldrich, Germany. Nanoparticle graphene nanoplatelets (GNPs) with a surface area of 300 m^2/g, bulk density of 200–400 kg/m^3 and particle size of <2 µm were acquired from US research Nanomaterials Inc. to further improve the thermal properties of the developed ternary eutectic PCMs.

2.2. Determination of Thermal Properties of Ternary Eutectic PCMs

The mixture of three different salt hydrate PCMs at different proportions formed ternary eutectic salt hydrate PCMs. For any PCM, T_m is isothermal in nature, and while developing a new eutectic PCM (mixing two or more pure PCMs with different T_m), a constant solitary melting point is very important. Henceforth, we adopted a numerical method to determine the proportion at which the salt hydrate PCMs (SCD, SSD and SPDD) had to be added for a common phase transition temperature of the developed ternary eutectic PCM. Based on the literature and reliability of Schrader' equation, we used Equation (1) derived as per phase equilibrium theory to determine the eutectic T_m and the eutectic mixture ratio. This numerical method reduced the number of tests required to determine the common melting point and is also an economical technique. As Schrader's equation [16] is well applied for a eutectic mixture of two components, we considered the property of two pure salt hydrate PCMs individually (component A and component B). Using Equation (1), we determined the eutectic melting point and their composition to develop a binary eutectic salt hydrate [17]. Later, considering the properties of the designated binary salt hydrate PCM as a single salt (component A), we included the third pure salt hydrate PCM (component B) to prepare the ternary eutectic salt hydrate PCM. Likewise, we used Equation (2) to determine the phase transition enthalpy of the designed ternary eutectic salt hydrate PCM [18].

$$T_m = \left[\frac{1}{T_i} - R\cdot\frac{\ln X_i}{\Delta H_{m,i}}\right]^{-1} \quad (1)$$

$$H_{eu} = T_{eu}\cdot\sum_{i=1}^{n}\left[\frac{X_i\cdot H_i}{T_i} + \left\{X_i\cdot\left(Cp_{li} - Cp_{si}\right)\cdot\ln\frac{T_{eu}}{T_i}\right\}\right] \quad (2)$$

In the equations above, T_m is the phase transition temperature of the eutectic mixture in K, T_i represents the phase transition temperature of individual salt hydrates (A, B, C) in K, the proportion of the individual salt hydrate mixture is represented as X in mole fraction. ΔH_m and ΔH_{eu} specify the melting enthalpy of pure and eutectic salt hydrate PCM, respectively, in $kJ.kmol^{-1}$, and R is the universal gas constant 8.314 $kJ{\cdot}mol^{-1}{\cdot}K^{-1}$. C_p represents the specific heat capacity in solid and liquid phases, respectively, in KJ/kgK.

2.3. Preparation of Ternary Eutectic PCMs

This section elaborates the step-by-step process of preparing the ternary eutectic PCM, and the nanoparticle-dispersed ternary eutectic salt hydrate PCM. The designed ternary salt hydrate PCMs of composition SCD/SPDD/SSD at weight fractions of x/y/z were prepared through melting followed by sonication. Figure 1 illustrates the step-by-step synthesis process of the ternary eutectic PCM, and the process of dispersing GNPs with a base ternary eutectic PCM. Based on the numerical design, we obtained the ternary eutectic composition of SCD/SPDD/SSD with the weight ratio of 44.8/21/34.2 and a melting point of 21.5 °C. At first, we melted 4.48 g of SCD salt hydrate PCM in a beaker using a hot plate maintained at 45 °C. Furthermore, 2.1 g of SPDD was added to the liquid phase SCD, and we obtained

a binary eutectic PCM (SCD/SPDD) with a melting point of 26.5 °C. As a final point, we mixed 3.42 g of SSD salt hydrate to the binary eutectic PCM, and hereby we prepared the designed ternary eutectic PCM (SCD/SPDD/SSD). To further enhance the thermal property of the prepared ternary eutectic salt hydrate PCM, GNPs were dispersed at different weight concentrations (0.4 wt%, 0.7 wt% and 1.0 wt%) and coded as SCD/SPDD/SSD-0.4GNP, SCD/SPDD/SSD-0.7GNP and SCD/SPDD/SSD-1.0GNP correspondingly. At the end, the composite samples were sonicated using an ultrasonicator bath (EASY 60H, ELMASONIC) for 30 min to ensure uniform dispersion of GNPs with the ternary eutectic PCM.

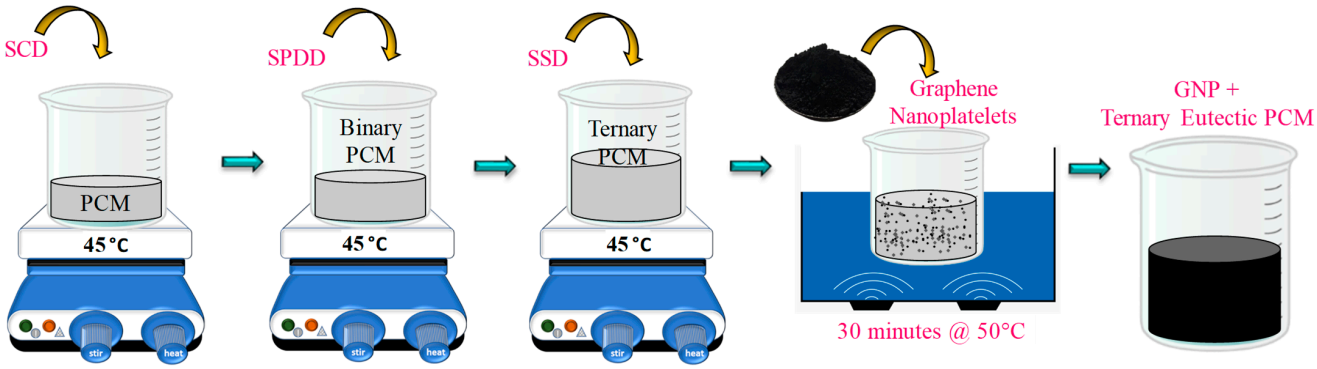


Figure 1. Synthesis of ternary eutectic salt hydrate PCM, with crystal structure visuals of pure salt hydrate PCM.

2.4. Instruments and Characterization Techniques

To characterize and experimentally evaluate the developed low-temperature ternary eutectic PCMs, we used a few sensitive instruments. The morphology of the individual pure salt hydrate PCMs was observed using an optical Stemi Microscope (Model STEMI2000, ZEISS). The microstructure of GNPs was examined with a scanning electron microscope (SEM) TESCAN VEGA 3. FT-IR spectroscopy (Perkin Elmer, Waltham, MA, USA) was used to detect spectral peaks of the ternary eutectic PCM and its composites with GNP. The wavenumber range of 400 to 4000 cm^{-1} was chosen to study the chemical composition, as the mid IR spectrum wavelength ranges between 2.5 and 25 µm. Optical absorbance and transmittance of the prepared sample in the solar spectrum region were examined using UV–vis spectroscopy (Model: LAMBDA 750, Perkin Elmer, USA). The readings were taken from a wavelength of 200 to 1400 nm at solid state. DSC instrument (DSC 3500 Sirius, NETZSCH) was used to analyze the melting temperature and latent heat properties of the TPCM composite. DSC melting and cooling curves were inspected between −15 and 45 °C under a N_2 atmosphere with a heating rate of 5 °C/min to determine the heating and cooling enthalpy, phase transition temperature and degree of supercooling. The base PCM and the developed nanocomposite PCM were numerically analyzed by ANSYS R16.0. All curves were plotted in Origin 2020 software.

3. Results and Discussion

A combination of numerical and experimental characterization was carried out in the current work. This research investigation was focused on developing a ternary eutectic salt hydrate PCM, designed to operate in low-temperature thermal energy regulation units. Here we designed, developed and characterize the synthesized ternary eutectic PCM with GNPs to ensure their chemical stability, optical absorptivity and thermal properties.

3.1. Design and Development of Ternary Eutectic Salt Hydrate PCM

Eutectic PCMs hold the advantage of tailoring the melting point of PCM as per the desired application. Here, a novel low-temperature ternary eutectic mixture PCM consisting of SCD, SPDD and SSD was designed numerically, followed by experimental synthesis and characterization for space cooling. Schrader's Equation (1) was chosen to numerically evaluate the eutectic weight ratio of the individual salt hydrate for obtaining a common

phase transition point. At first, we considered the thermal properties of salt hydrate SCD (T_m = 31 °C; ΔH_m = 210 J/g) and SPDD (T_m = 37 °C; ΔH_m = 227 J/g) to evaluate the binary eutectic phase transition temperature (T_{eu}). The fraction of salt hydrate (X_i) in Equation (1) was varied to determine T_{eu}. On evaluation, it was observed that a binary eutectic mixture of SCD and SPDD exhibited a common phase transition temperature at 26.1 °C. Figure 2a represents T_{eu} of SCD/SPDD at different weight proportions, and it can be inferred that T_{eu} (26.1 °C) was obtained with 32% of SPDD and 68% of SCD. The obtained eutectic point is a temperature at which the individual component both starts to melt and undergoes phase transition. Eutectic phase transition temperature is always lower than the phase transition temperature of the individual component, owing to the increase in impurity (inclusion of another component), where entropy generation increases and tends to reduce the melting point of the mixture [19,20]. Both individual components undergo a decrease in temperature and converge at a common point, which is the eutectic point. Likewise, using Equation (2), we determined the heat storage enthalpy of the developed binary eutectic PCM. Figure 2b depicts the variation in the latent heat value of pure salt hydrate PCM and binary eutectic PCM at different weight compositions. On further calculation, the latent heat of the binary eutectic PCM was determined to be 210 J/g.

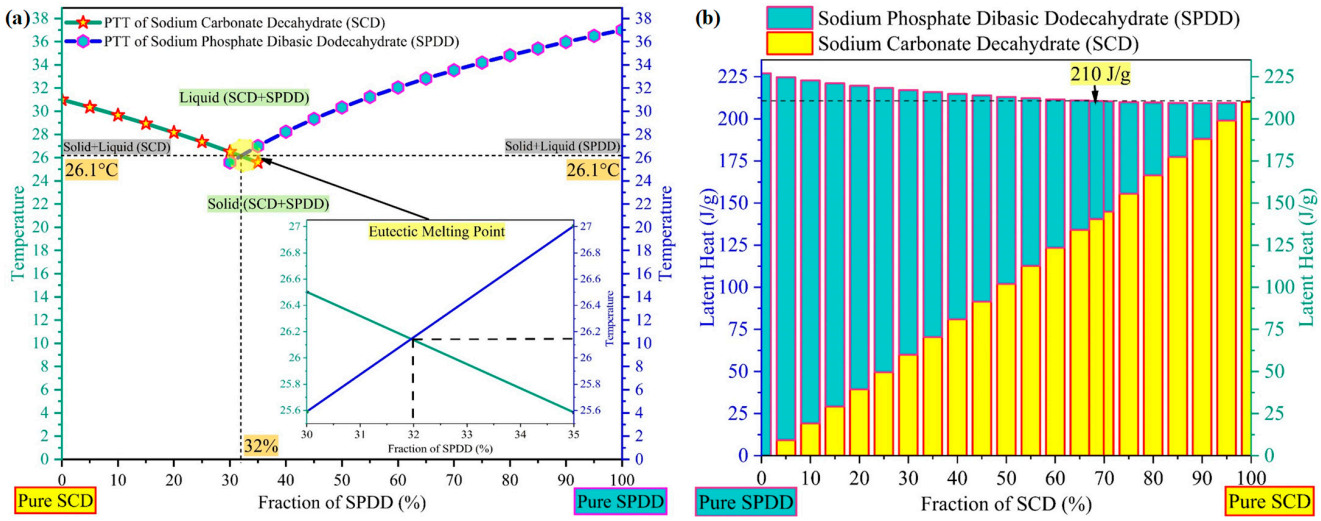


Figure 2. (**a**) Phase transition point of SCD/SPDD binary salt hydrate PCM; (**b**) heat storage enthalpy of SCD/SPDD binary salt hydrate PCM.

Considering the binary eutectic PCM SSD/SPDD (T_m = 26.1 °C; ΔH_m = 210 J/g) as a unique salt hydrate PCM (individual component) and pure SSD (T_m = 33 °C; ΔH_m = 217 J/g) salt hydrate PCM (second component), we adopted Equations (1) and (2) to calculate the eutectic melting point, composition ratio and latent heat for the ternary eutectic PCM. Figure 3a,b describes the variation in melting point and latent heat of the eutectic PCM, with variation in proportion of the component. On evaluation, it was observed that the ternary eutectic mixture of SCD, SPDD and SSD exhibited a common phase transition temperature at 21.5 °C. From Figure 3a it can be inferred that the eutectic phase transition temperature 21.5 °C was obtained at 34.2% of SSD and 65.8% of SCD/SPDD. SCD/SPDD exhibited a eutectic melting point at 68% of SCD and 32% of SPDD. Henceforth it was determined that the composition of the developed ternary eutectic PCM was 34.2% SSD, 44.75% SCD (65.8% of 68%SCD) and 21.05% SPDD (65.8% of 32%SPDD). Likewise, for SCD/SPDD/SSD (34.2/21.05/44.75), the latent heat value was determined to be 207 J/g.

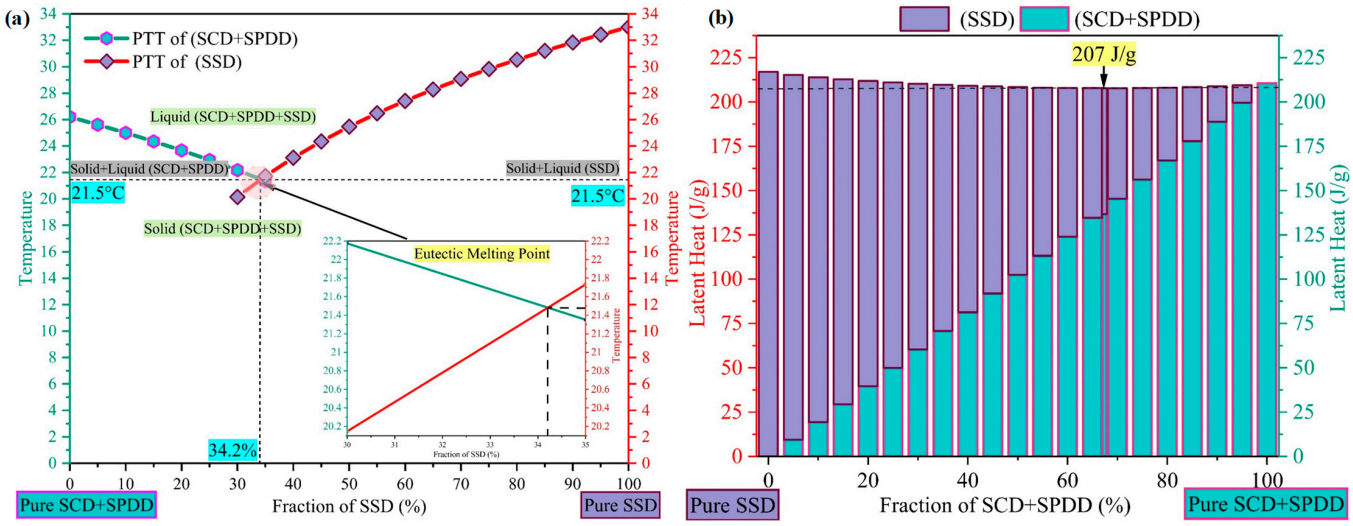


Figure 3. (**a**) Phase transition point of SCD/SPDD/SSD binary salt hydrate PCM; (**b**) heat storage enthalpy of SCD/SPDD/SSD binary salt hydrate PCM.

3.2. Morphological Behavior

The microstructure and morphology of the developed inorganic-salt-hydrate-based ternary eutectic PCM was examined using an optical microscope. Figure 4 shows the optical image visuals of pure salt hydrate SCD, SPDD and SSD for a better understanding on the crystal structure (bulk, coarse and fine). SCD salt hydrate displayed very fine salt crystals of uniform size, whereas SPDD salt hydrate PCM consisted of bulk and coarse salt crystals with irregular shape. Although SPDD is a dodecahydrate molecule, due to a high melting temperature (37 °C), the salt hydrate is complete in the solid state, without exhibiting any water molecule presence in the surface like SCD. On keen observation it could be inferred that the developed binary eutectic PCM (SCD/SPDD) and the ternary eutectic PCM (SCD/SPDD/SSD) replicated a uniform morphology in terms of the crystal structure and grain size and ensured a proper dispersion. High hydrated molecules of SCD/SPDD/SSD were also understandable from the optical visual image. The morphology and microstructure of nanoparticle GNPs were examined using a scanning electron microscope (SEM), and the images are provided in Figure 4. It can be inferred that GNP nanomaterials had two-dimensional irregular multiple layers of a sheet-like structure with some voids and gaps between subsequent layers. Nevertheless, we depicted the digital image of the base ternary eutectic PCM and GNP-dispersed ternary eutectic PCM for better consideration of the dispersion of GNP with the developed ternary eutectic PCM.

3.3. Chemical Stability

On investigating the developed ternary eutectic PCM under a FTIR spectrometer, the wavelength position and intensity of the absorption band imitated the characteristics of molecular structure, which is significant in understanding the presence of a chemical group. FTIR spectral curves of the developed ternary eutectic PCM (SCD/SPDD/SSD) and its composites with different fractions of GNP can be observed from Figure 5. In all the tested samples, we could observe wide and sharp spectral peaks with varying intensity. The wide peak around wavenumber 2900–3600 cm^{-1} represented the O-H stretching vibration due to the crystallization of water molecules [21]. Sharp peaks at wavenumber 990 cm^{-1} denoted the PO-H [22] bending vibration, ensuring the presence of the SPDD salt hydrate. The sharp peak at 1077 cm^{-1} represented SO_4^{2-} [23], with asymmetric stretching vibration ensuring the presence of the SSD salt hydrate. The other higher intense sharp peak at 1383 cm^{-1} represented CO_3^{2-} [24], indicating the asymmetric stretching vibration confirming the presence of the SCD component. Additionally, GNPs under exposure to the FTIR spectrum do not produce any peaks within the IR range, which ensures the non-IR active nature

of GNPs [25]. In all the spectral curves of GNP-dispersed ternary eutectic PCM, no new absorption peaks were generated, and there were no missing peaks that were observed in the ternary eutectic PCM. This spectral curve as obtained from FTIR ensured that no chemical reaction occurred between the developed ternary eutectic PCM GNP at different concentrations due to any physical interaction.

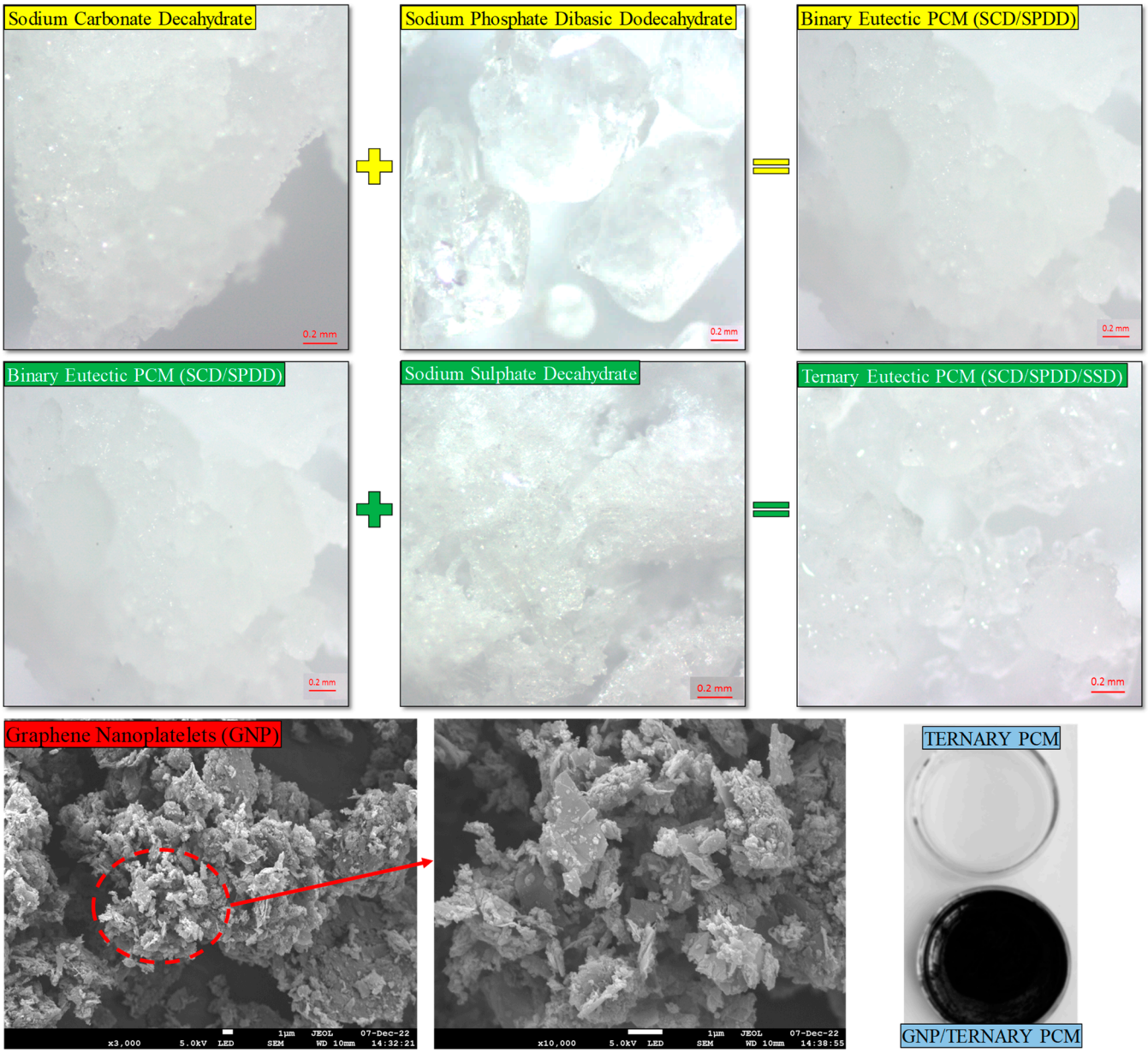


Figure 4. Crystal structure visuals of pure and eutectic salt hydrate PCM using an optical microscope; microstructure and morphological image of graphene nanoplatelets; and digital image of base ternary eutectic composite and GNP-dispersed ternary eutectic composite.

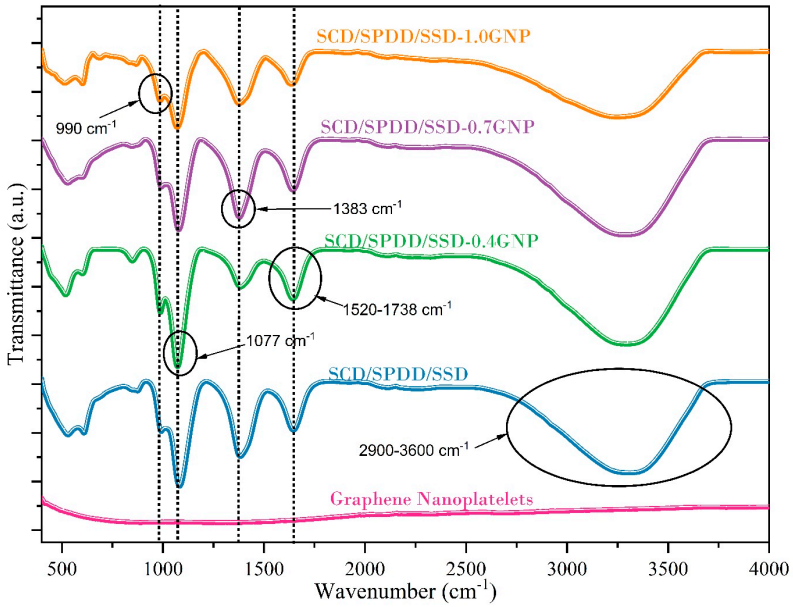


Figure 5. FTIR spectral curves of ternary eutectic PCM and GNP-dispersed ternary eutectic PCM.

3.4. Optical Property Analysis

The developed ternary eutectic PCM was designed to be operated for thermal regulation of buildings. PCM melting at 21.5 °C can be preferably used for building heating as well as building cooling. In general, for building heating, heat energy from solar power is absorbed and stored in the PCM, and later this energy is released into the heating space for thermal regulation [26]. On analysis it is noted that most of the inorganic materials are transparent and transmit more solar radiation than absorption. Hence in this section, the optical property of the developed ternary eutectic salt hydrate PCM was experimentally investigated under UV–vis spectroscopy. Figure 6a,b shows the absorbance and transmittance curves of the developed ternary eutectic salt hydrate PCM along with GNP at different weight concentrations with variation in ultraviolet–visible light waves.

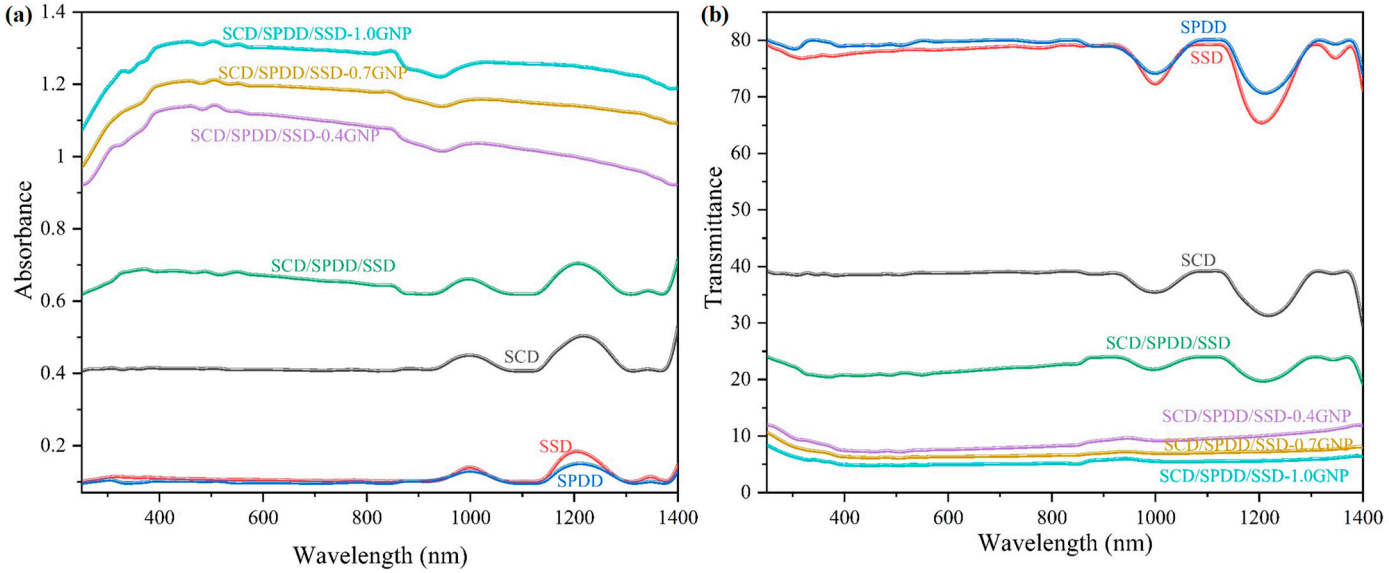


Figure 6. Solar spectral (**a**) absorbance and (**b**) transmittance of GNP-dispersed ternary eutectic PCM.

As can be seen in Figure 6a, the absorbance intensity of the developed ternary eutectic PCM SCD/SPDD/SSD (0.62 absorbance) was stronger in comparison with that of the individual salt hydrate PCM SCD (0.43 absorbance), SPDD (0.14 absorbance) and SSD (0.15 absorbance) in all regions (UV and visible). The higher optical absorptivity of SCD/SPDD/SSD could be ascribed to the stickier nature of the developed ternary PCM with higher content of water molecules. The crystal structures also contributed towards repeated scattering within the PCM and enhanced the absorptivity. In addition, the improvement in optical properties with dispersion of GNPs was further inferred. Spectral curves of GNP-dispersed SCD/SPDD/SSD at nanoparticle concentrations of 0.4%, 0.7% and 1.0% illustrated absorbances of 1.02, 1.18 and 1.28, respectively. Increases in optical absorptivity of GNP-dispersed ternary PCM were ascribed to the dark nature of the GNP-dispersed composite. The dark nature decreased the transmissibility of the PCM and improved the absorptivity. Besides absorbance, the transmissibility behavior of the developed ternary PCM is depicted in Figure 6b. The lower the transmittance, the better the absorbance. On further assessment, the optical absorptivity of the ternary salt hydrate PCM reduced from 21.8% to 8.4%, 6.7% and 5.2% for GNP weight concentrations of 0.4, 0.7 and 1.0, respectively. Greater absorptivity improves the solar energy input and contributes to higher TES at a comparatively faster rate.

3.5. Thermal Conductivity

PCM for any application is selected based on the heat energy storage potential and the rate at which the thermal energy charging takes place. Thermal conductivity indicates the rate at which the heat transfer occurs in any materials. In general, inorganic PCM offers improved thermal conductivity compared to that of organic PCM. Although this research work focuses on inorganic PCMs, to further increase the thermal properties of the developed ternary eutectic salt hydrate PCM, we dispersed 2D GNPs at concentrations of 0.4%, 0.7% and 1.0% to evaluate the thermal property enhancement.

As the developed ternary eutectic PCM was designed to operate at a low temperature, we used a transient hot-bridge thermal conductivity meter to find the thermal conductivity of the GNP-dispersed ternary eutectic PCM and the pure salt hydrate PCMs. The room temperature was maintained at 15 °C to ensure a solid state of the sample while conducting the characterization experiment. Figure 7 shows the bar plots of pure salt hydrate SCD, SPDD and SCD; developed ternary eutectic PCM SCD/SPDD/SSD and GNP-dispersed ternary eutectic PCM at different compositions. In solid materials, the significant cause for thermal conductivity is the movement of free electrons; however, inorganic salt hydrates have fewer free electrons as most of the electrons remain confined to the ionic crystal lattice [3]. Hence in inorganic salt hydrates, thermal conduction occurs due to crystal lattice vibration. Figure 7 depicts the thermal conductivity of base salt hydrate PCM SCD, SSD and SPDD as 0.441 W/m·K, 0.458 W/m·K and 0.513 W/m·K, respectively. As a new ternary eutectic PCM was developed, it was of utmost importance to evaluate the thermal conductivity of the synthetic PCM with their individual mixtures. The thermal conductivity of the synthesis PCM was 0.473 W/m·K, which was a nominal value between the thermal conductivity of SCD and SPDD, which could be ascribed to the distribution of the base salt hydrate. Furthermore, GNPs were dispersed at weight concentrations of 0.4%, 0.7% and 1.0% to advance the thermal conductivity of the synthesized PCM. It can be inferred that 0.4%, 0.7% and 1.0% of GNPs enhanced the thermal conductivity of the ternary PCM by 31.7%, 48.6% and 71.5%, respectively. The increment in thermal conductivity was ascribed to higher thermal conductivity of the GNPs and their higher surface area, which develops a well-connected thermal network for enhanced heat transfer rate [26]. On the whole, comparing the thermal conductivity (0.811 W/m·K) of SCD/SPDD/SSD-0.7GNP PCM with that of organic PCM (0.2 W/m·K), there was an increment of nearly 300%.

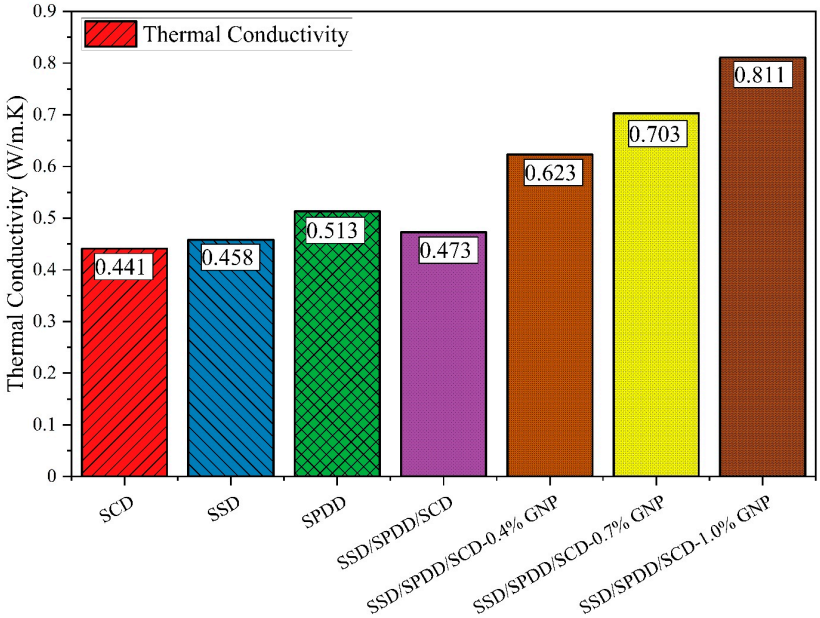


Figure 7. Thermal conductivity of GNP-dispersed ternary eutectic salt hydrate PCM.

3.6. Melting Temperature, Latent Heat Storage and Degree of Supercooling

PCM are preferred for TES owing to their ability to store higher energy within a small mass of PCM. Inorganic PCMs also offer the benefits of higher latent heat potential compared to that of organic PCMs. This section consolidates and compares the experimentally determined melting point, latent heat and degree of supercooling of the GNP-dispersed ternary eutectic PCM. To begin with, we compared the latent heat (207 J/g) value and melting temperature (21.5 °C) of the numerically designed ternary eutectic PCM in Section 3.1 with those of the experimentally determined PCM using a DSC instrument. Figure 8 shows the experimentally determined endothermic peaks of pure salt hydrate PCM (SCD, SPDD and SSD) and the binary eutectic PCM (SCD/SPDD). With further calculation it could be inferred that the latent heat values of SCD, SSD and SPDD salt hydrate were 208.2 J/g, 216.2 J/g and 226.1 J/g, respectively. All the experimental latent heat values were like the numerical values used for designing the binary and ternary eutectic PCMs. Similarly, the latent heat value of the binary eutectic PCM was 210.3 J/g, which was like the numerically calculated latent heat (210 J/g). The melting temperature of the binary eutectic PCM was inferred to be 25.6 °C and closely resembled the T_m of SCD/SPDD binary eutectic PCM designed based on Schrader's equation. Figure 9a shows the experimentally tested endothermic peak of the SCD/SPDD/SSD ternary eutectic PCM with heat storage potential of 203.2 J/g and a melting point of 21.3 °C. It was also observed that the eutectic points of the developed binary and ternary eutectic PCMs were lower compared to that of the individual salt hydrate, which was ascribed to the increase in impurity, where entropy generation increased and reduced the melting point of the mixture. It was also noticed that the latent heat value of the ternary eutectic PCM was slight lower than the numerical calculated value; the explanation to be noted is the increase in free energy (ΔG°) due to the impure solid (mixture of two or more components), causing entropy generation resulting in a slight reduction of latent heat of the prepared eutectic PCM. This experimental investigation ensured the reliability of Schrader's equation in developing a new eutectic PCM for TES.

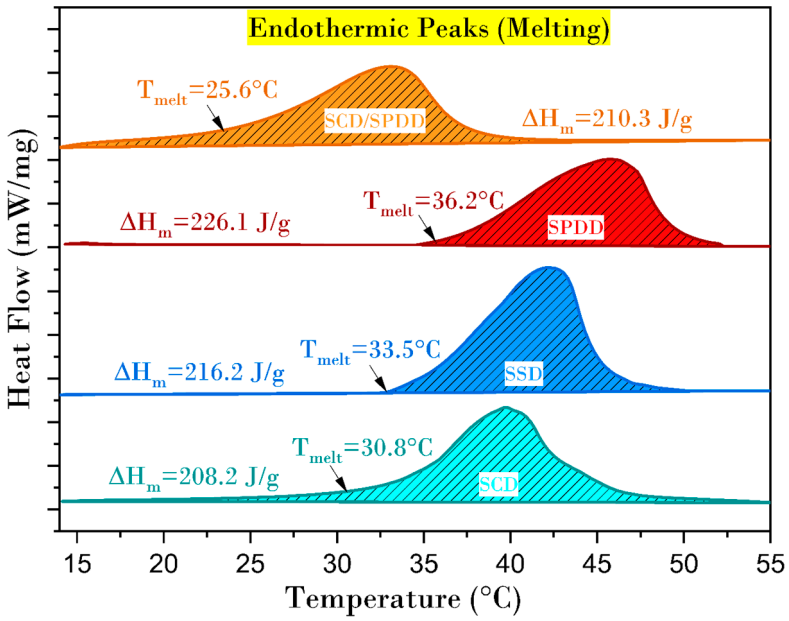


Figure 8. Heat storage enthalpy of pure salt hydrate PCM and binary eutectic salt hydrate PCM.

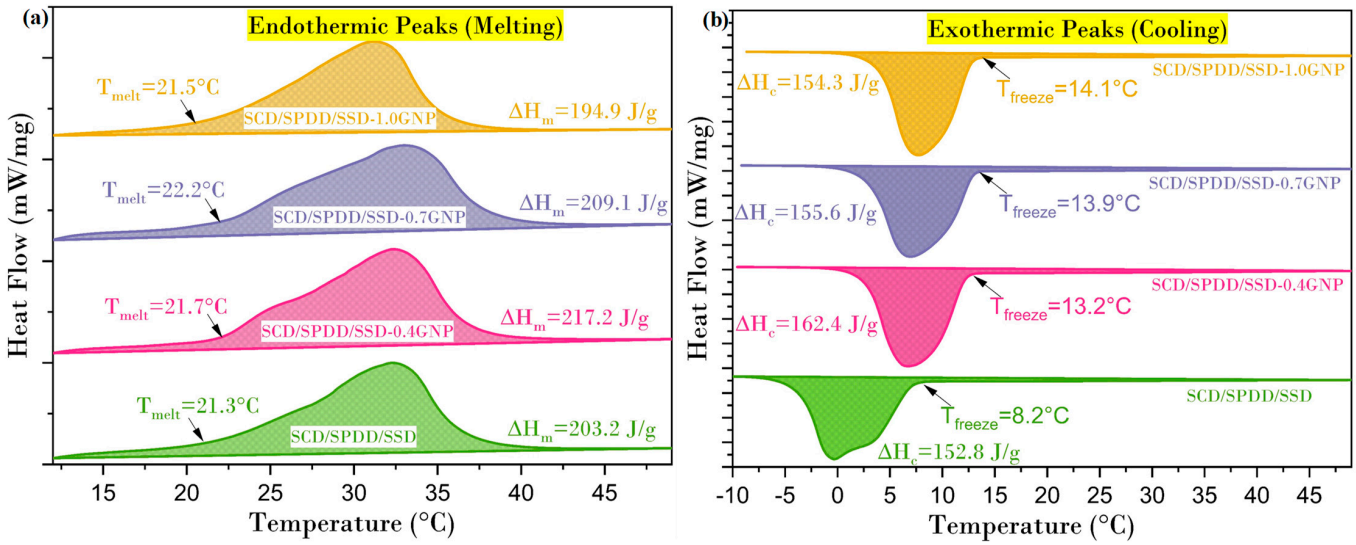


Figure 9. Heat storage enthalpy of GNP-dispersed eutectic salt hydrate PCM; (**a**) melting curve and (**b**) cooling curve.

DSC curves in Figure 9 depict the heating and cooling pattern of the ternary eutectic PCM and the GNP-dispersed ternary eutectic PCM. Three parameters to be discussed and inferred are (a) melting point, (b) heat storage enthalpy and (c) degree of supercooling. The developed ternary eutectic PCM was a combination of three different salt hydrates with melting points ranging between 31 and37 °C. Nevertheless, the synthesized eutectic PCM exhibited a single melting peak, which ensured the solid-to-liquid phase transition with uniform dispersion of the salt hydrate and the reliability of Schrader's equation. The ternary eutectic PCM's (SCD/SPDD/SSD) melting began at 21.3 °C, which was more like the numerically calculated eutectic point. The lower eutectic point of the developed PCM was due to the increase in impurity of the composition. On dispersion of GNPs, the melting point of the PCM increased slightly as the nanoparticles contributed towards higher thermal conductivity. Nevertheless, the phase transition temperature of the GNP-dispersed ternary eutectic PCM as in the range of 21.7–22.2 °C and is preferred for the thermal regulation of buildings.

Subsequently, the melting enthalpy and cooling enthalpy of the GNP-dispersed ternary eutectic PCMs were portrayed well in Figure 9a,b. It could be inferred that the melting enthalpies of the developed PCM with 0.4%, 0.7% and 1.0% of GNPs were 217.2 J/g, 209.1 J/g and 194.9 J/g, respectively. Latent heat describes the stronger intermolecular force of attraction between the PCM molecules. On the whole, the inclusion of nanoparticles with PCM increases the intermolecular attraction between the molecules of PCM and nanoparticles and accounts for storing higher heat energy. The increase in latent heat of the GNP-dispersed PCM was ascribed to the higher surface area of GNPs, which improved the intermolecular force of attraction between the nanoparticle and the ternary eutectic PCM. Nevertheless, the nanoparticle also replaced the mass of the PCM, and the material's ability to store heat energy drops at a higher concentration. Hence, at a low concentration of nanoparticles, the intermolecular interactions are dominant, and at a higher concentration, the drop in latent heat is accounted for by the mass of nanoparticles replacing the mass of PCM [27]. Likewise, the cooling plot in Figure 9b depicts that about 162.4 J/g, 155.6 J/g and 154.3 J/g of energy could be extracted from the energy that was stored during phase transition of the GNP-dispersed PCM from the liquid to solid state. On evaluation, the energy storage efficiency was 75.56% for the base ternary eutectic PCM, 75.46% for SCD/SPDD/SSD-0.4GNP, 74.0% for SCD/SPDD/SSD-0.7GNP and 78.4% for SCD/SPDD/SSD-1.0GNP.

One more important parameter to discuss with salt hydrate PCMs is their degree of supercooling (difference in temperature between the actual freezing point of PCM and the point at which PCM actually freezes). The major hindrance with usage of salt hydrate PCMs is their concern towards the issue of supercooling. During the phase transition of PCMs from liquid to solid state, they are expected to freeze at the temperature at which the PCM starts melting. With most salt hydrates failing to crystallize at their melting point, it reduced the heat storage ability. In this experimental investigation, the degree of supercooling was calculated as the difference in temperature between T_{melt} and T_{freeze}. From Figure 9a,b it was found that the degree of supercooling of the ternary eutectic PCM and its GNP-dispersed composite at concentrations of 0.4%, 0.7% and 1.0% were 13.1 °C, 8.5 °C, 8.3 °C and 7.4 °C, respectively. Although nucleating agents were not included in this investigation, GNPs performed the role of the nucleating agent and reduced the degree of supercooling by 35.2%, 36.655% and 43.52% with 0.4%, 0.7% and 1.0% weight concentrations, respectively.

3.7. Numerical Analysis of Ternary Eutectic PCM

A separate heat transfer analysis on the ternary eutectic PCM and GNP-dispersed PCM was conducted based on different heat energy input supply as in Figure 10. In this evaluation, we created a circular 2D enclosure to better understand the energy storage unit. Initially, we considered a circular PCM layer with their circumference open to a heat sink for constant heat input. The 2D PCM enclosure was maintained at a temperature of 20 °C, and the heat sink temperature was varied as 25, 30 and 35 °C, which was above the melting point (>21.6 °C) of the GNP-dispersed ternary eutectic PCM. We analyzed the developed ternary eutectic PCM with thermal conductivity of 0.473 W/m.K and 1.0 weight concentrated GNP-dispersed ternary eutectic PCM with thermal conductivity of 0.811 W/m.K.

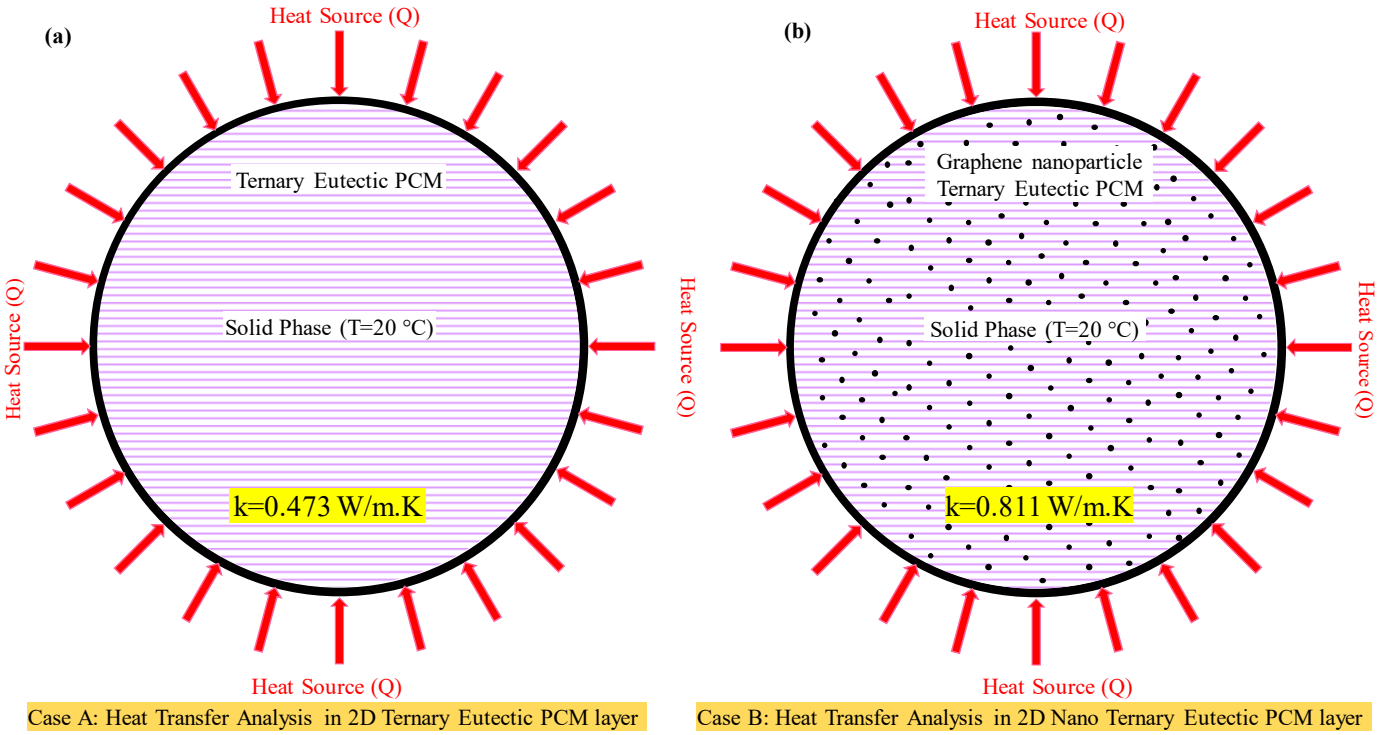


Figure 10. Boundary condition depiction of heat transfer investigation; (**a**) ternary eutectic PCM layer and (**b**) GNP-dispersed ternary eutectic PCM layer.

This numerical analysis as per the boundary condition in Figure 10 emphasizes the thermal energy propagation over the ternary eutectic PCM and GNP eutectic PCM. The heat transfer with temperature contour plots of the base and GNP-composite ternary eutectic PCMs with input heat energies of 40, 45 and 50 °C is shown in Figure 11. We conducted a steady-state heat transfer analysis for a circular PCM layer, with heat supply throughout the circumference layer. As the developed ternary eutectic PCM was specifically opted for low-temperature analysis, we supplied a low heat input with a temperature range of 40, 45 and 50 °C. Two major parameters to discuss are the thermal property of the PCM layer and the variation in supplied heat. It can be inferred from Figure 11a–c that with an increase in input energy source, the heat transfer and depth of penetration varied; however, the temperature change between the PCM and heat input was very minimal. The color scale depicts the heat penetration of the PCM. Likewise, enhancement of thermal conductivity with GNP dispersion further improved the heat penetration rate, which is clearly understandable from Figure 11 d–f. On analysis it was observed that for effective heat penetration the input source needed to be enhanced predominantly.

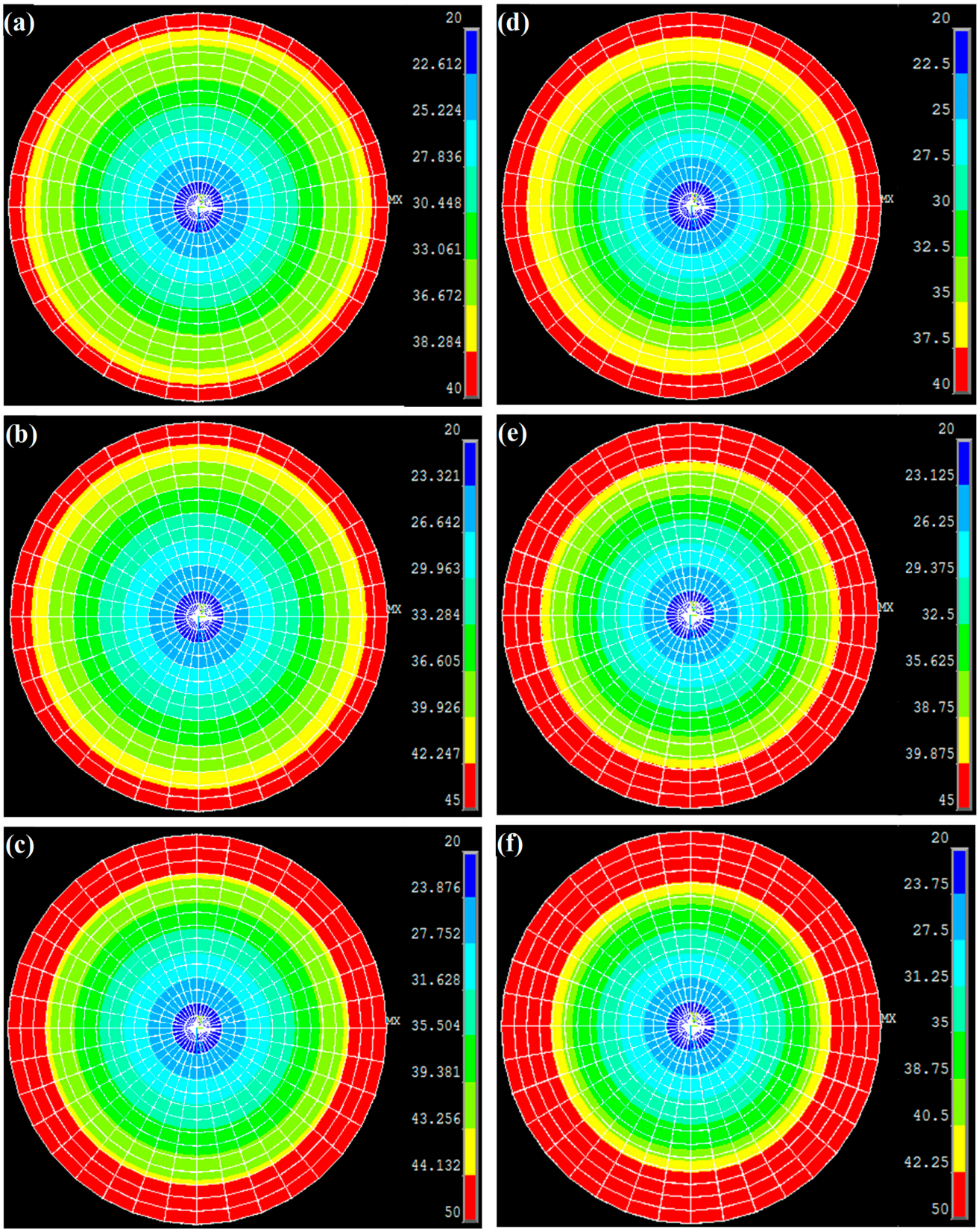


Figure 11. Temperature contour plots of ternary eutectic PCM with heat source of (**a**) 40 °C, (**b**) 45 °C (**c**) and 50 °C; and of 1.0 GNP-dispersed ternary eutectic PCM at heat input source of (**d**) 40 °C, (**e**) 45 °C and (**f**) 50 °C.

4. Conclusions

Energy storage using a eutectic salt hydrate is reliable with tailored thermal properties as per the desired application. In this current research work, a ternary eutectic salt hydrate PCM was designed numerically and developed experimentally to characterize its thermal properties. Ternary eutectic PCM SCD/SPDD/SCD showed a phase transition temperature of 21.5 °C, latent heat storage of 207 J/g, thermal conductivity of 0.473 W/m·K and optical absorptivity of 0.62 with a lower degree of supercooling compared to that of the individual salt hydrate. The developed ternary eutectic PCM was further investigated with dispersion of GNP and different weight concentrations. The results showed an increase in thermal conductivity and optical absorbance by 71.5% and 106.5%, respectively. Likewise, the degree of supercooling and transmissibility were reduced by 43.5% and 76.2% correspondingly. The GNP-dispersed composite ternary eutectic PCM was chemically stable and also exhibited a better enhancement in thermal and optical properties. The integration of PCMs with buildings to regulate effective utilization of thermal energy will contribute towards sustainable development.

Author Contributions: Conceptualization, B.K. and A.K.P.; Data curation, B.K.; Formal analysis, B.K.; Funding acquisition, A.K.P. and S.R.; Investigation, B.K., A.K.P. and V.V.T.; Methodology, B.K.; Project administration, A.K.P., S.R. and K.S.; Resources, A.K.P.; Supervision, S.R., K.S. and V.V.T.; Validation, B.K.; Writing—original draft, B.K.; Writing—review & editing, A.K.P., S.R. and V.V.T. All authors have read and agreed to the published version of the manuscript.

Funding: The authors acknowledge the financial assistance of Sunway University through Sunway University's International Research Network Grant Scheme 2.0 (IRNGS 2.0) 2021 (STR-IRNGS-SET-RCNMET-01-2021) for carrying out this research.

Institutional Review Board Statement: Not Applicable.

Informed Consent Statement: Not Applicable.

Data Availability Statement: The data presented in this study is available within the article.

Conflicts of Interest: The authors declare no conflict of interest.

References

1. Yu, K.; Liu, Y.; Yang, Y. Review on form-stable inorganic hydrated salt phase change materials: Preparation, characterization and effect on the thermophysical properties. *Appl. Energy* **2021**, *292*, 116845. [CrossRef]
2. Kalidasan, B.; Pandey, A.; Shahabuddin, S.; Samykano, M.; Thirugnanasambandam, M.; Saidur, R. Phase change materials integrated solar thermal energy systems: Global trends and current practices in experimental approaches. *J. Energy Storage* **2020**, *27*, 101118.
3. Kalidasan, B.; Pandey, A.; Saidur, R.; Samykano, M.; Tyagi, V. Nano additive enhanced salt hydrate phase change materials for thermal energy storage. *Int. Mater. Rev.* **2022**, 1–44. [CrossRef]
4. Chen, W.; Liang, X.; Wang, S.; Ding, Y.; Gao, X.; Zhang, Z.; Fang, Y. SiO_2 hydrophilic modification of expanded graphite to fabricate form-stable ternary nitrate composite room temperature phase change material for thermal energy storage. *Chem. Eng. J.* **2021**, *413*, 127549. [CrossRef]
5. Tian, H.; Du, L.; Wei, X.; Deng, S.; Wang, W.; Ding, J. Enhanced thermal conductivity of ternary carbonate salt phase change material with Mg particles for solar thermal energy storage. *Appl. Energy* **2017**, *204*, 525–530. [CrossRef]
6. Wang, T.; Mantha, D.; Reddy, R.G. Novel high thermal stability LiF–Na_2CO_3–K_2CO_3 eutectic ternary system for thermal energy storage applications. *Sol. Energy Mater. Sol. Cells* **2015**, *140*, 366–375. [CrossRef]
7. Liang, L.; Chen, X. Preparation and thermal properties of eutectic hydrate salt phase change thermal energy storage material. *Int. J. Photoenergy* **2018**, *2018*, 6432047. [CrossRef]
8. Sun, W.; Huang, R.; Ling, Z.; Fang, X.; Zhang, Z. Two types of composite phase change panels containing a ternary hydrated salt mixture for use in building envelope and ventilation system. *Energy Convers. Manag.* **2018**, *177*, 306–314. [CrossRef]
9. Efimova, A.; Pinnau, S.; Mischke, M.; Breitkopf, C.; Ruck, M.; Schmidt, P. Development of salt hydrate eutectics as latent heat storage for air conditioning and cooling. *Thermochim. Acta* **2014**, *575*, 276–278. [CrossRef]
10. Zhang, N.; Yuan, Y.; Wang, X.; Cao, X.; Yang, X.; Hu, S. Preparation and characterization of lauric–myristic–palmitic acid ternary eutectic mixtures/expanded graphite composite phase change material for thermal energy storage. *Chem. Eng. J.* **2013**, *231*, 214–219. [CrossRef]

11. Jebasingh, B.E. Preparation of organic based ternary eutectic fatty acid mixture as phase change material (PCM), optimizing their thermal properties by enriched solar treated exfoliated graphite for energy storage. *Mater. Today Proc.* **2016**, *3*, 1592–1598. [CrossRef]
12. Zhang, W.; Zhang, X.; Huang, Z.; Yin, Z.; Wen, R.; Huang, Y.; Wu, X.; Min, X. Preparation and characterization of capric-palmitic-stearic acid ternary eutectic mixture/expanded vermiculite composites as form-stabilized thermal energy storage materials. *J. Mater. Sci. Technol.* **2018**, *34*, 379–386. [CrossRef]
13. Ke, H. Investigation of the effects of nano-graphite on morphological structure and thermal performances of fatty acid ternary eutectics/polyacrylonitrile/nano-graphite form-stable phase change composite fibrous membranes for thermal energy storage. *Sol. Energy* **2018**, *173*, 1197–1206. [CrossRef]
14. Luo, Z.; Zhang, H.; Gao, X.; Xu, T.; Fang, Y.; Zhang, Z. Fabrication and characterization of form-stable capric-palmitic-stearic acid ternary eutectic mixture/nano-SiO_2 composite phase change material. *Energy Build.* **2017**, *147*, 41–46. [CrossRef]
15. He, Q.; Fei, H.; Zhou, J.; Du, W.; Pan, Y.; Liang, X. Preparation and characteristics of lauric acid-myristic acid-based ternary phase change materials for thermal storage. *Mater. Today Commun.* **2022**, *32*, 104058. [CrossRef]
16. Nazir, H.; Batool, M.; Ali, M.; Kannan, A.M. Fatty acids based eutectic phase change system for thermal energy storage applications. *Appl. Therm. Eng.* **2018**, *142*, 466–475. [CrossRef]
17. Ke, H. Phase diagrams, eutectic mass ratios and thermal energy storage properties of multiple fatty acid eutectics as novel solid-liquid phase change materials for storage and retrieval of thermal energy. *Appl. Therm. Eng.* **2017**, *113*, 1319–1331. [CrossRef]
18. Du, W.; Fei, H.; Pan, Y.; He, Q.; Zhou, J.; Liang, X. Development of capric acid-stearic acid-palmitic acid low-eutectic phase change material with expanded graphite for thermal energy storage. *Constr. Build. Mater.* **2022**, *320*, 126309. [CrossRef]
19. Nordlie, B. *Eutectic Melting. Petrology*; Kluwer Academic Publishers: Dordrecht, The Netherlands, 1989; pp. 155–157.
20. Nichols, L. *Organic Chemistry Laboratory Techniques*; Independent: Chicago, IL, USA, 2016.
21. Lin, N.; Li, C.; Zhang, D.; Li, Y.; Chen, J. Emerging phase change cold storage materials derived from sodium sulfate decahydrate. *Energy* **2022**, *245*, 123294. [CrossRef]
22. Shen, Z.; Oh, K.; Kwon, S.; Toivakka, M.; Lee, H.L. Use of cellulose nanofibril (CNF)/silver nanoparticles (AgNPs) composite in salt hydrate phase change material for efficient thermal energy storage. *Int. J. Biol. Macromol.* **2021**, *174*, 402–412. [CrossRef]
23. Zhang, Z.; Lian, Y.; Xu, X.; Xu, X.; Fang, G.; Gu, M. Synthesis and characterization of microencapsulated sodium sulfate decahydrate as phase change energy storage materials. *Appl. Energy* **2019**, *255*, 113830. [CrossRef]
24. Nickolov, Z.S.; Ozcan, O.; Miller, J. FTIR analysis of water structure and its significance in the flotation of sodium carbonate and sodium bicarbonate salts. *Colloids Surf. A Physicochem. Eng. Asp.* **2003**, *224*, 231–239. [CrossRef]
25. Kumar, R.; Samykano, M.; Ngui, W.; Pandey, A.; Kalidasan, B.; Kadirgama, K.; Tyagi, V. Investigation of thermal performance and chemical stability of graphene enhanced phase change material for thermal energy storage. *Phys. Chem. Earth Parts A/B/C* **2022**, *128*, 103250. [CrossRef]
26. Kalidasan, B.; Pandey, A.; Rahman, S.; Yadav, A.; Samykano, M.; Tyagi, V. Graphene–Silver Hybrid Nanoparticle based Organic Phase Change Materials for Enhanced Thermal Energy Storage. *Sustainability* **2022**, *14*, 13240. [CrossRef]
27. Wang, F.; Zheng, W.; Gou, Y.; Jia, Y.; Li, H. Thermal behaviors of energy storage process of eutectic hydrated salt phase change materials modified by Nano-TiO_2. *J. Energy Storage* **2022**, *53*, 105077. [CrossRef]

Disclaimer/Publisher's Note: The statements, opinions and data contained in all publications are solely those of the individual author(s) and contributor(s) and not of MDPI and/or the editor(s). MDPI and/or the editor(s) disclaim responsibility for any injury to people or property resulting from any ideas, methods, instructions or products referred to in the content.